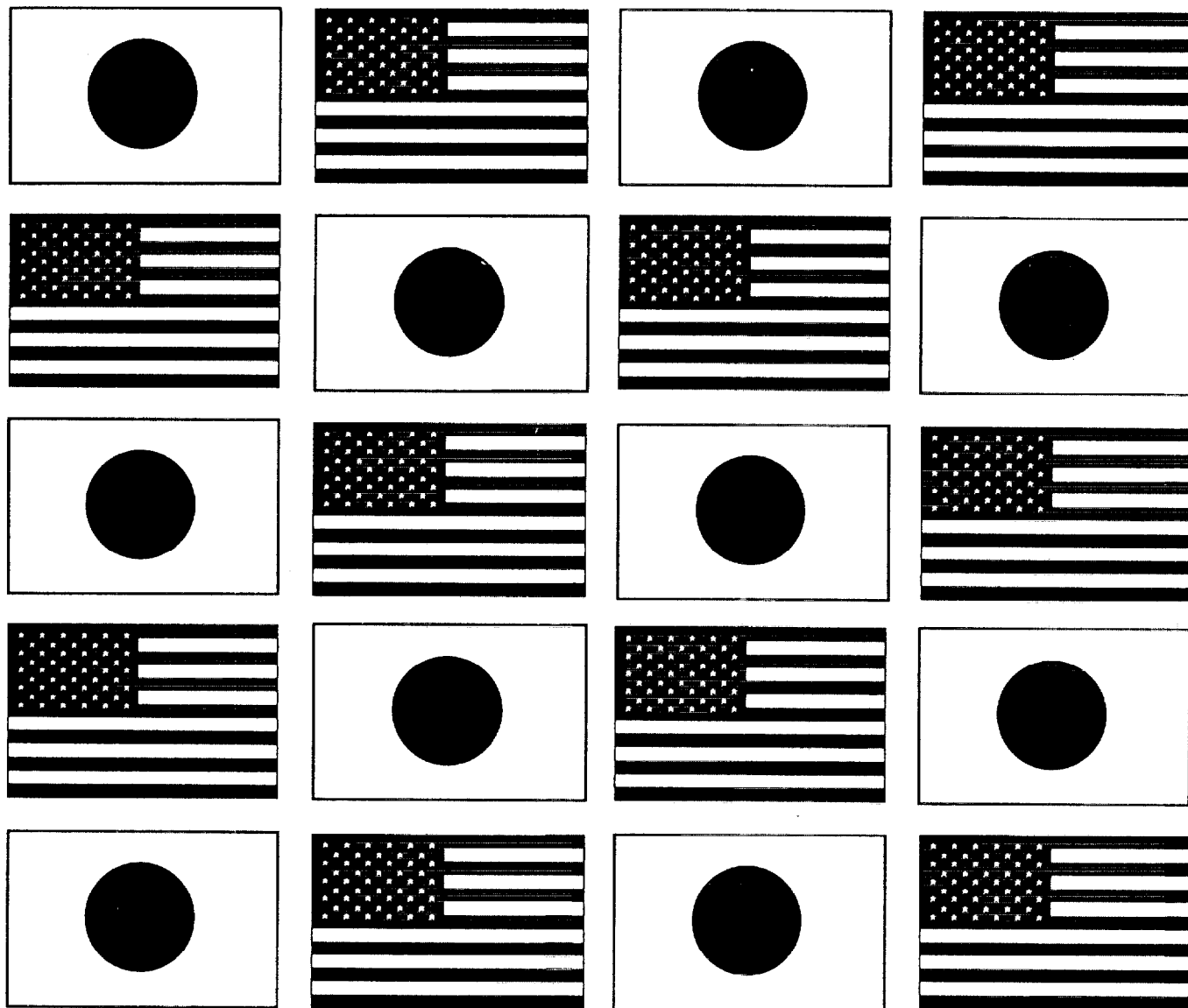


Wind and Seismic Effects

Proceedings of the 30th Joint Meeting

NIST SP 931



U.S. DEPARTMENT OF COMMERCE
Technology Administration
National Institute of Standards and Technology

Wind and Seismic Effects

NIST SP 931

**PROCEEDINGS OF
THE 30TH JOINT
MEETING OF
THE U.S.-JAPAN
COOPERATIVE PROGRAM
IN NATURAL RESOURCES
PANEL ON WIND AND
SEISMIC EFFECTS**

Issued August 1998

**Noel J. Raufaste
EDITOR**

**Building and Fire Research Laboratory
National Institute of Standards and Technology
Gaithersburg, MD 20899**



**U.S. DEPARTMENT OF COMMERCE
William M. Daley, Secretary**

**TECHNOLOGY ADMINISTRATION
Gary R. Bachula, Acting Under Secretary for Technology**

**National Institute of Standards and Technology
Raymond G. Kammer, Director**

**MANUSCRIPTS AUTHORED for
PANEL MEETING but NOT
PRESENTED ORALLY**

Aerodynamic databases and electronic standards for wind loads: A pilot application

by

Timothy Whalen^{1,2}, Emil Simiu¹, Gilliam Harris³, Jason Lin⁴, and David Surry⁴

ABSTRACT

As part of ongoing National Institute of Standards and Technology research on the development of a new generation of standard provisions for wind loads, we present results of a pilot project on the use of large aerodynamic databases for the improved estimation of wind-induced bending moments and shear forces in low-rise building frames. We use records of wind pressure time histories measured at a large number of taps on the building surface in the Boundary Layer Wind Tunnel of the University of Western Ontario. Time histories of moments and shear forces in a frame are obtained by adding pressures at all taps tributary to that frame multiplied by the respective tributary areas and influence coefficients. The latter were obtained from frame designs provided by CECO Building Systems. We compare results obtained by using the pressure time history records with results based on ASCE 7 standard provisions. The comparison shows clearly that provisions which use aerodynamic databases containing the type of data described in this work can result in designs that are significantly more risk-consistent as well as both safer and more economical than designs based on conventional standard provisions. We outline future research on improved design methodologies made possible by our proposed approach to wind loading standardization. Finally, the proposed methodologies may be used for damage assessment for insurance purposes.

KEYWORDS: Building technology; aerodynamics; codes and standards; databases; risk; structural engineering; wind engineering.

1. INTRODUCTION

Conventional standard provisions for wind loads

reflect two conflicting needs: (1) to assure that they are risk-consistent, the provisions should reflect the information on which they are based as completely and realistically as possible; and (2) conventional standards have limitations that impose reductive formats and simplifications, with consequent loss of information and risk-consistency.

Owing to current information storage and computational capabilities standard provisions need no longer be based on reductive -- and distorting -- tables and plots. It is now practical to develop user-friendly standard provisions that incorporate large amounts of useful information [1,2]. In this paper we present results that illustrate aspects of the development and advantages of such provisions in the specific case of low-rise building frames.

In Section 2 we describe (1) the geometry of the buildings chosen as our test cases, (2) the design criteria for the frames, and (3) basic information on the frames, which were designed by CECO Building Systems. In Section 3 we briefly describe the wind tunnel tests performed at the Boundary Layer Wind Tunnel Laboratory of the University of Western Ontario (BLWTL) [3]. In Section 4 we describe the procedure used to calculate wind-induced internal forces (i.e., bending moments, shear forces and axial forces),

¹Building and Fire Research Laboratory, National Institute of Standards and Technology, Gaithersburg, MD 20899

²Present address: School of Civil Engineering, Purdue University, West Lafayette, IN 47907

³CECO Building Systems, Columbus, MS 39703

⁴Boundary Layer Wind Tunnel Laboratory, University of Western Ontario, London, Ont., Canada N6A 5B9

using: (1) the ASCE 7-93 Standard provisions on wind loads [4], and (2) time-dependent loads based on the wind tunnel measurements. In Section 5 we present and discuss our results. In Section 6 we discuss the vast potential for improving both the safety and economy of structural designs offered by the approach described in this paper, and future research aimed at realizing that potential.

2. BUILDING GEOMETRIES, DESIGN CRITERIA, AND FRAMES

The buildings studied in this pilot project are rectangular in plan with dimensions 61 m (200 ft) \times 30.5 m (100 ft), and have gable roofs with 1/24 slopes and ridge parallel to the long dimension. For the first set the eave height is $H=6.1$ m (20 ft); for the second set it is $H=9.75$ m (32 ft). Each set consists of four buildings with identical geometry. Two of the four buildings are located near Miami, Florida. The other two are located near Charleston, S.C. For each of these locations one building is in open terrain and one is in suburban terrain. All buildings are located at 13 km (8 miles) inland from the coastline and are assumed to be Category 1 [4].

The frames were designed by CECO Building Systems in accordance with Metal Buildings Manufacturers Association (MBMA) current practices, which are based on the the ASCE 7-93 Standard and the 1989 AISC Design Manual (Allowable Stress Design). The configuration of the frames is shown in Fig. 1. For the direction normal to the ridge, the main wind load resisting systems consist of 2 end frames and 7 interior frames. The distance between interior frames is 7.62 m (25 ft) center to center. The end frames are equally spaced from the respective neighboring interior frame. The frame dimensions and the cross-sectional dimensions of the webs and flanges are identical for all frames of a given building. We refer to the Miami (M) building with $H=6.1$ m (20 ft) in suburban (S) terrain as MS20. The other buildings are designated MS32, CS20, CS32, and MO20, MO32, CO20, CO32 (C designates Charleston;

O designates open terrain).

3. WIND TUNNEL TESTS

Building models were tested at 1:200 and 1:100 scales for suburban terrain and 1:200 scale for open terrain. Pressure taps were installed at about 500 locations for the buildings with $H=9.75$ m and 440 locations for the buildings with $H=6.1$ m. The tap locations are shown in Fig. 2. Pressure time histories were measured for each of 37 wind directions between 0° and 180° at 5° intervals. Pressure coefficients C_p obtained from the pressure measurements were referenced to the experimental dynamic pressures at the eave height H . The approximate wind tunnel mean flow speeds $V_h(H)$ at the model eave height H correspond to the full-scale hourly speeds listed in Table 1.

In this paper we consider only the 1:200 model tests. The characteristics of the wind tunnel flows conform to standard representations of atmospheric boundary-layer flows over open and suburban terrain -- see [3] for details.

The time series were sampled at 400 Hz for 60 s. The processed time series were corrected for residual non-simultaneity, and digitally low-pass filtered at 150 Hz. The resolution for the pressure coefficients is about 0.01. The data were archived onto 8 mm cassette tapes. Each tape contains two directories. Each directory contains all the data for one building with specified eave height in one type of terrain. The size of a directory is about 2 GigaBytes when uncompressed and about 600 MegaBytes when compressed. For details on the data file structure and on restoring data from tapes see [3].

4. WIND-INDUCED INTERNAL FORCES

Wind-induced internal forces were obtained for two types of wind loadings: (1) the wind loading specified by the ASCE 7-93 Standard and (2) the wind loading obtained from the wind tunnel data. The ASCE loading is based on wind speeds estimated without regard for direction. For

consistency our estimates of the wind loading obtained from wind tunnel tests are based on similar estimates of the wind speeds. The pressures are

$$p(t) = 0.613 C_p(t) V_h^2(H) \quad (\text{N/m}^2) \quad (1)$$

$$V_h(H) = 1.046 (K_z)^{1/2} V c, \quad (2)$$

where C_p is the pressure coefficient as determined from the wind tunnel tests, 1.046 is the importance factor for Category 1 buildings located at 13 km (8 miles) from the coastline (Table 5 of [4]), H is the eave height in meters, $V_h(H)$ is the mean hourly speed at elevation H , V is the basic wind speed in m/s ($V = 42.5$ m/s (95 mph) for Charleston and 49.6 m/s (111 mph) for Miami -- see Fig. 1 of [4]), K_z is an exposure coefficient whose square root transforms the fastest-mile wind speed at 10 m elevation over open terrain into the fastest-mile wind speed at elevation H over the specified type of terrain (for $H = 6.1$ m (20 ft), $K_z = 0.87$ for open terrain and $K_z = 0.42$ for suburban terrain; for $H = 9.75$ m (32 ft), $K_z = 0.996$ for open terrain and $K_z = 0.514$ for suburban terrain -- see Table 6 of [4]), and c is a coefficient that transforms fastest-mile wind speeds to mean hourly speeds ($c \approx 1/1.30$ for Charleston and $c \approx 1/1.31$ for Miami -- see Sect. 6.5.2.2 and Fig. C5 of the Commentary in [4]).

The internal forces were obtained by summing up the pressures at all taps contributing to the loading of a frame times the respective tributary area and influence coefficient. The influence coefficients were calculated using standard linear analysis techniques, and accounted for the position of the tap with respect to the frame. It was assumed that the load associated with any given tap is transmitted to the frame by simply supported girts or purlins, and that there is no load redistribution among the frames. For the loading based on wind-tunnel results this procedure yielded time histories of the internal forces being sought, from which r.m.s. values of the internal forces were obtained. The internal force corresponding to a nominal one-hour loading is defined as the mean value plus the

r.m.s. value times the peak factor

$$k_{pk} = (2 \ln 3600 v_p)^{1/2} + 0.577 / (2 \ln 3600 v_p)^{1/2} \quad (3)$$

[5], where v_p is the mean zero upcrossing rate of the fluctuating part (excluding the mean) of the internal force for the prototype. The rate v_p is obtained from its model counterpart by equating reduced frequencies for the model and prototype. This yields $v_m/v_p = \{[V_h(H)]_m/[V_h(H)]_p\}(D_p/D_m)$, where the subscripts p and m indicate model and prototype, respectively, and D_p/D_m is the reciprocal of the model scale. The speed $V_h(H)$ for the model is taken from Table 1. It is assumed that the wind speed specified by the ASCE 7-93 Standard can blow from any direction.

5. RESULTS

For 6 cross-sections shown in Fig. 1, Table 2 lists the ratio between the worst case bending moments induced by the time-dependent load modeled on the basis of the wind tunnel tests (for brevity, we will refer to this load as the actual loading) and their counterpart worst case bending moments induced by ASCE Standard 7-93 loads. In both cases the respective most unfavorable wind loading conditions were assumed. If the loading specified by the Standard were "on target", i.e., if it reflected consistently the actual loading, then all entries in Table 2 would be unity. Such consistency is impossible owing to the constraints imposed on the volume of information that can be conveyed in conventional standard provisions. Given those constraints the ASCE 7-93 Standard writers attempted to specify information as consistently as possible. However, we note that for any given frame the ratios of Table 2, instead of being unity, differ significantly and nonuniformly from unity in most cases. For example, for the frames of building CS20, the ratios vary from a minimum of 0.5 to a maximum of 0.82. This means that some cross-sections will be more over-designed than others. The sections that are the most over-designed contribute little to the overall safety of the frame. The statement can

therefore be made -- conditional on the strength having a given value -- that the least over-designed cross-section would fail if a sufficiently powerful storm occurred, with the additional strength reserve of the more over-designed cross-sections being wasted. The ratio between the maximum and the minimum entry for a given type of frame is denoted by r_i , and is a measure of the inconsistency of the design over the cross-sections listed in Table 2 for that type of frame. We also list in Table 2 the ratio, denoted by r_{inf} , between the maximum to the minimum entry across types of frames for cross-sections #2, #4, and # 6 (these sections are the section at the frame knee, girder pinch, and ridge line, where comparisons between frame types are meaningful). The ratio r_{inf} is a measure of the extent to which the influence lines of the frames affect the capability of the conventional standard provisions to reflect the actual moments occurring in the frames. This capability is affected by the fact that the standard provisions were based on one specific type of influence lines. Inconsistencies between effects of loads in conventional standard provisions and effects of actual loads inevitably arise should the design of the frames deviate from the design assumed in development of the conventional standard provisions. It can be seen in Table 2 that r_{inf} can be as large as 1.52. (We also note that the ASCE standard does not differentiate between loads on two-hinged and three-hinged frames, even though the respective influence lines are significantly different. Nor does the ASCE 7 standard make allowance for the distance between frames, even though owing to the fluctuating nature of the loads this distance can affect significantly the magnitude of the internal forces.)

The adoption of standard provisions that use large aerodynamic databases would result in moment and shear diagrams allowing the designs would be risk-consistent both within a frame and across different frames. The waste inherent in non-uniformities within a frame would therefore be eliminated. For example, for frame CS32, the design would be safer if instead of the ratio 1.00 (for cross-section #6), the ratio 0.9 were used,

and it would also be more economical if the ratios 0.65, 0.67, 0.74, 0.58, and 0.87 were to be changed to the ratio 0.9.

Design technology has progressed to the point where designers can achieve designs with stresses that are within a few percentage points of the stresses induced by the standard loads. However, this close match provides only the illusion of good design, since the designer is deprived by conventional standard provisions of the knowledge of the actual loads and the associated actual stresses. A standard using large aerodynamic databases would allow the designer to design for the best available loading information that can be produced in the present state of the art, without the significant artificial distortions due to the conventional standards' antiquated way of conveying loading information.

Since the present investigation is exploratory, we considered only wind directions 0° , 30° , 60° , 90° , and 120° . In a forthcoming report all 37 wind directions will be considered. Preliminary searches have indicated that consideration of the results for all 37 directions will leave Table 2 essentially unchanged.

6. FUTURE RESEARCH

As already indicated, the aim of this paper is to present a pilot study. An exhaustive investigation along the lines presented in this paper is planned, however, which will include consideration of all wind directions. It will also consider the effects of wind directionality, which we assumed here to be characterized by a circular extreme wind rosette. This assumption is used in the ASCE 7-93 Standard, but it is fact not necessarily warranted, as shown by the example of the wind rosette of Fig. 3 (milepost 1950, near Charleston, see [6]). We plan to investigate the effect of modeling scale using the results obtained in the wind tunnel for 1:100 models. Instead of estimating moments for a few selected sections, we plan to produce full moment and shear force diagrams for the entire frames. It is conceivable that automated production will render desirable in

the future designs that may be somewhat different for the various frames of a given building. Moment and shear force diagrams corresponding to various mean recurrence intervals can be produced for each of those individual frames, giving the designer the option of considering the possibility of reducing the amount of material for some frames, if this is warranted by the moment and shear force diagrams.

We also plan to study the possibility of automated iterative designs, starting with a design based, for example, on conventional standard provisions, refining the design on the basis of moment and shear diagrams based on actual wind loads, recalculating the moments and shears based on the influence lines of the new frame, until a satisfactory convergence is achieved. Only then will designs accommodating calculated stresses to within a few percentage points make sense, that is, offer the substance rather than the illusion of good engineering design. We note that anticipated progress in Computational Fluid Dynamics might allow the entire load definition process to be computerized in the future, at least for certain applications. Finally, we note that the power of the computer and the availability of databases for time histories of wind pressures make it possible for researchers and designers to study the plastic behavior of frames in the time domain on the basis of realistic fluctuating wind loads. Plastic designs are currently viewed by the industry as uneconomical, and allowable stress designs are used instead, but further research made possible by the availability of appropriate databases containing aerodynamic pressure time histories will enable research to be conducted that might lead to a change of current design philosophy.

7. REFERENCES

1. Simiu, E. and Stathopoulos, T. (1997), "Codification of wind loads on buildings using bluff body aerodynamics and climatological data bases," *J. Wind Eng. Ind. Aerodyn.* (in press).
2. Simiu, E., Garrett, J.H., and Reed, K.A. (1993), "Development of Computer-based Models of Standards and Attendant Knowledge-base and Procedural Systems," in *Struct. Eng. In Natural Hazards Mitigation, Structures Congress*, Irvine, Calif., American Society of Civil Engineers, New York.
3. Lin, J. and Surry, D. (1997), *Simultaneous Time Series of Pressures on the Envelope of Two Large Low-rise Buildings*, BLWT-SS7-1997, Boundary-Layer Wind Tunnel Laboratory, The Univ. of Western Ontario, London, Ontario, Canada.
4. *ASCE Standard 7-93* (1993), American Society of Civil Engineers, New York.
5. Davenport, A.G. (1964), "Note on the Distribution of the Largest Values of a Random Function with Application to Gust Loading," *J. Inst. Civ. Eng.* **24**, 187-196.
6. Simiu, E. and Scanlan, R.H. (1996), *Wind Effects on Structures: Fundamentals and Applications to Design*, 3rd Ed., Wiley-Interscience, New York.

Table 1. Wind tunnel mean flow speeds $V_h(H)$

| | |
|--|-----------|
| 1:200 model, open terrain, H=6.10 m: | 10.15 m/s |
| 1:200 model, open terrain, H=9.75 m: | 10.95 m/s |
| 1:200 model, suburban terrain, H=6.10 m: | 8.30 m/s |
| 1:200 model, suburban terrain, H=9.75 m: | 8.95 m/s |
| 1:100 model, suburban terrain, H=6.10 m: | 9.35 m/s |
| 1:100 model, suburban terrain, H=9.75 m: | 10.05 m/s |

Table 2. Ratios of maximum moments due to loads modeled by wind tunnel data to moments induced by ASCE 7-93 Standard provisions, for six frame cross-sections

| Frame for building type | CS20 | CO20 | CS32 | CO32 | MS20 | MO20 | MS32 | MO32 | r_{inf} |
|----------------------------|------|------|------|------|------|------|------|------|-----------|
| Cross-section (see Fig. 1) | | | | | | | | | |
| #1 | 0.60 | 0.61 | 0.75 | 0.65 | 0.60 | 0.61 | 0.74 | 0.62 | |
| #2 | 0.66 | 0.66 | 0.78 | 0.66 | 0.65 | 0.66 | 0.78 | 0.67 | 1.20 |
| #3 | 0.75 | 0.76 | 0.89 | 0.74 | 0.75 | 0.75 | 0.87 | 0.73 | |
| #4 | 0.50 | 0.46 | 0.68 | 0.58 | 0.51 | 0.52 | 0.70 | 0.67 | 1.52 |
| #5 | 0.79 | 0.76 | 0.90 | 0.87 | 0.78 | 0.75 | 0.89 | 0.86 | |
| #6 | 0.82 | 0.79 | 1.00 | 0.96 | 0.81 | 0.78 | 0.98 | 0.85 | 1.28 |
| $r_f = r_{max}/r_{min}$ | 1.64 | 1.72 | 1.47 | 1.66 | 1.59 | 1.50 | 1.40 | 1.39 | |

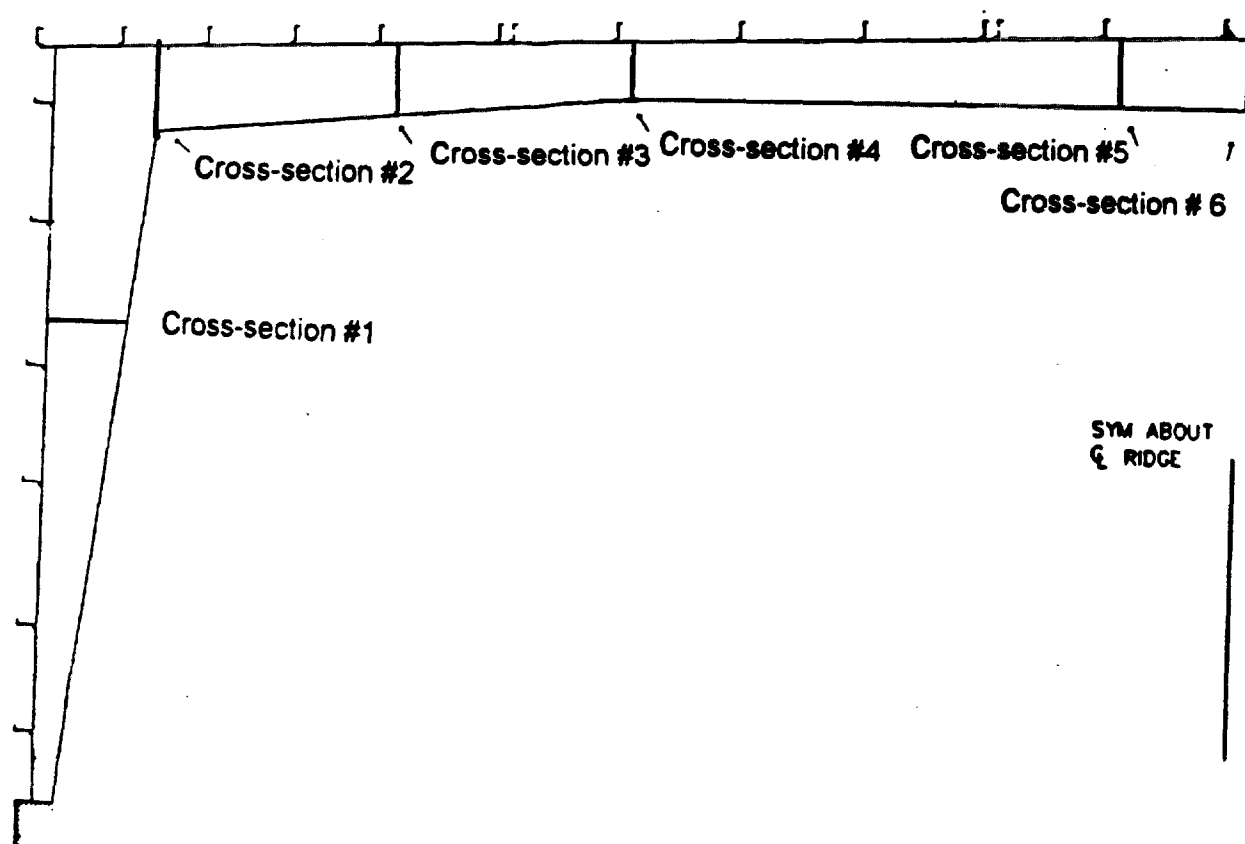
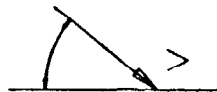


Fig. 1. Schematic of typical frame taken from construction drawing.



| | | | | |
|-----|-----|-----|-----|-----|
| 105 | 104 | 103 | 102 | 101 |
| 106 | 107 | 108 | 109 | 110 |
| 115 | 114 | 113 | 112 | 111 |
| 116 | 117 | 118 | 119 | 120 |
| 209 | 208 | 207 | 206 | 205 |
| 210 | 211 | 212 | 213 | 214 |
| 303 | 302 | 301 | 300 | 299 |
| 304 | 305 | 306 | 307 | 308 |
| 313 | 312 | 311 | 310 | 309 |
| 314 | 315 | 316 | 317 | 318 |
| 407 | 406 | 405 | 404 | 403 |
| 408 | 409 | 410 | 411 | 412 |
| 501 | 502 | 503 | 504 | 505 |
| 506 | 507 | 508 | 509 | 510 |

SIDEWALL 24

| | | | | | | | | | | | | | |
|------|------|------|------|------|------|------|------|------|------|------|------|------|------|
| 1003 | 1002 | 1709 | 1708 | 1615 | 1614 | 1605 | 1604 | 1510 | 1509 | 1416 | 1415 | 1406 | 1405 |
| 1004 | 1001 | 1710 | 1707 | 1616 | 1613 | 1606 | 1603 | 1511 | 1508 | 1501 | 1414 | 1407 | 1404 |
| 1005 | 1716 | 1711 | 1706 | 1701 | 1612 | 1607 | 1602 | 1512 | 1507 | 1502 | 1413 | 1408 | 1403 |
| 1006 | 1715 | 1712 | 1705 | 1702 | 1611 | 1608 | 1516 | 1513 | 1506 | 1503 | 1412 | 1409 | 1402 |
| 1007 | 1714 | 1713 | 1704 | 1703 | 1610 | 1609 | 1515 | 1514 | 1505 | 1504 | 1411 | 1410 | 1401 |

| | | | | | | | | | | | | | |
|-----|------|------|------|------|------|------|------|------|------|------|------|------|------|
| 200 | 2001 | 2100 | 2200 | 2300 | 2400 | 2500 | 2600 | 2700 | 2800 | 2900 | 3000 | 3100 | 3200 |
| 202 | 2102 | 2202 | 2302 | 2402 | 2502 | 2602 | 2702 | 2802 | 2902 | 3002 | 3102 | 3202 | |
| 203 | 2103 | 2203 | 2303 | 2403 | 2503 | 2603 | 2703 | 2803 | 2903 | 3003 | 3103 | 3203 | |
| 204 | 2104 | 2204 | 2304 | 2404 | 2504 | 2604 | 2704 | 2804 | 2904 | 3004 | 3104 | 3204 | |
| 205 | 2105 | 2205 | 2305 | 2405 | 2505 | 2605 | 2705 | 2805 | 2905 | 3005 | 3105 | 3205 | |
| 206 | 2106 | 2206 | 2306 | 2406 | 2506 | 2606 | 2706 | 2806 | 2906 | 3006 | 3106 | 3206 | |
| 207 | 2107 | 2207 | 2307 | 2407 | 2507 | 2607 | 2707 | 2807 | 2907 | 3007 | 3107 | 3207 | |
| 208 | 2108 | 2208 | 2308 | 2408 | 2508 | 2608 | 2708 | 2808 | 2908 | 3008 | 3108 | 3208 | |
| 209 | 2109 | 2209 | 2309 | 2409 | 2509 | 2609 | 2709 | 2809 | 2909 | 3009 | 3109 | 3209 | |
| 210 | 2110 | 2210 | 2310 | 2410 | 2510 | 2610 | 2710 | 2810 | 2910 | 3010 | 3110 | 3210 | |
| 211 | 2111 | 2211 | 2311 | 2411 | 2511 | 2611 | 2711 | 2811 | 2911 | 3011 | 3111 | 3211 | |
| 212 | 2112 | 2212 | 2312 | 2412 | 2512 | 2612 | 2712 | 2812 | 2912 | 3012 | 3112 | 3212 | |
| 213 | 2113 | 2213 | 2313 | 2413 | 2513 | 2613 | 2713 | 2813 | 2913 | 3013 | 3113 | 3213 | |
| 214 | 2114 | 2214 | 2314 | 2414 | 2514 | 2614 | 2714 | 2814 | 2914 | 3014 | 3114 | 3214 | |
| 215 | 2115 | 2215 | 2315 | 2415 | 2515 | 2615 | 2715 | 2815 | 2915 | 3015 | 3115 | 3215 | |

NUMBER OF TAPS
 ROOF 14x15 = 210
 SIDEWALLS 14x15x2 = 140
 ENDBALLS 15x5x2 = 150

TOTAL 500

| | | | | | | | | | | | | | |
|-----|-----|-----|-----|-----|-----|-----|-----|-----|-----|-----|-----|-----|-----|
| 506 | 506 | 506 | 506 | 506 | 506 | 506 | 506 | 506 | 506 | 506 | 506 | 506 | 506 |
| 512 | 603 | 604 | 611 | 612 | 703 | 704 | 711 | 712 | 803 | 804 | 811 | 812 | 904 |
| 513 | 602 | 605 | 610 | 613 | 702 | 705 | 710 | 713 | 802 | 805 | 810 | 813 | 903 |
| 514 | 601 | 606 | 609 | 614 | 701 | 706 | 709 | 714 | 801 | 806 | 809 | 814 | 902 |
| 515 | 506 | 607 | 608 | 615 | 616 | 707 | 708 | 715 | 716 | 807 | 808 | 815 | 901 |

Fig. 2. Schematic showing arrangement of pressure taps.

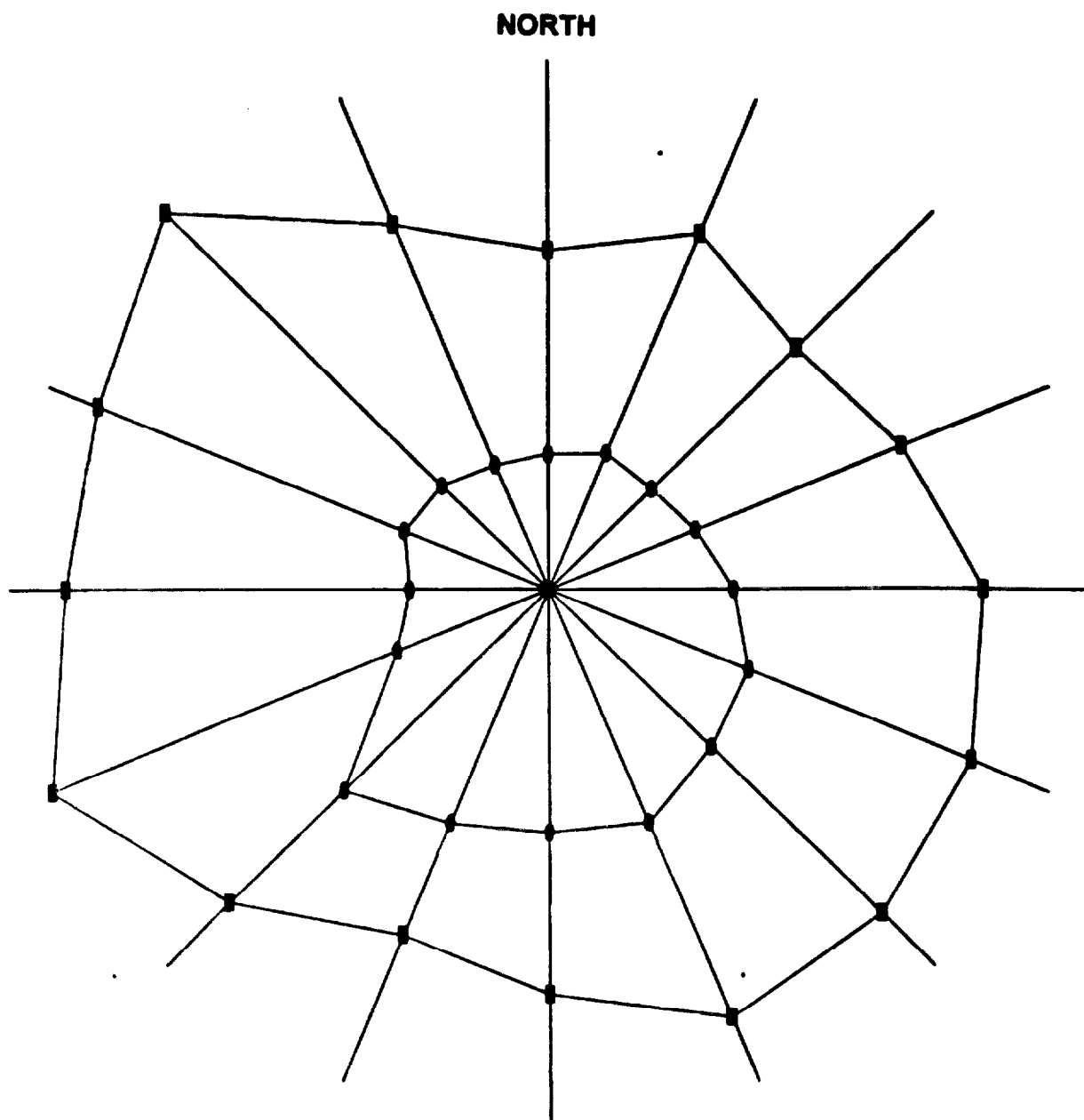


Fig. 3. Maximum and mean hurricane winds for 16 azimuths near Charleston, S.C. Largest directional speeds are 50 m/s (WSW and NW directions.)